Parameter Identification of the Planar Integrated EMI Filter Based on the Improved Immune Algorithm

Jinjun Bai, Hong Zhao*, Yulei Liu, and Kaibin Guo

College of Marine Electrical Engineering
Dalian Maritime University, Dalian, 116026, China
baijinjun@dlmu.edu.cn, zhaohong@dlmu.edu.cn, lyl15056811702abc@163.com, guokaibin112233@163.com

Abstract ─ The planar integrated EMI filter has been widely used because of its small size and good high-frequency characteristics. During the production process, if the electrical parameters of the integrated LC structure can be accurately identified, it will help improve the high-frequency characteristics of the filter. However, this identification problem is a multi-peak problem, which can easily fall into a local optimal solution. Based on the Feature Selective Validation method, this paper proposes an improved Immune Algorithm. The proposed method keeps changing the fitness function in the iterative process to avoid the algorithm falling into the local optimal solution. Finally, comparing with the measured impedance characteristic curve, it is verified that the proposed method is more accurate than the common Immune Algorithm.

Index Terms ─ Feature selective validation, immune algorithm, parameter identification, planar integrated EMI filter.

I. INTRODUCTION

In 2003, Chen from Virginia University of Technology proposed the Planar Electromagnetic Integration technology and applied it to Electromagnetic Interference (EMI) filter design [1,2]. The Planar Integrated EMI filter uses thin film technology to connect cores with different permeability to the printed circuit board, and the integrated LC (means inductance and capacitance) structure is formed to realize the filtering function. Its advantages are small size, easy modularization, and high frequency performance.

In 2013, Huang from South China University of Technology proposed common mode windings overlapped and interleaved layout technology, in order to improve the high frequency performance of the planar integrated EMI filter [3]. In 2014, Wang from Nanjing University of Aeronautics and Astronautics devised ring EMI filter structure. Using axisymmetric electrostatic field model and harmonic magnetic field model, the theoretical analysis of its electromagnetic characteristics has been realized [4]. In recent years, integrated EMI filters have been widely used in engineering practice, especially the design of DC–DC Power Electronic Converter [5, 6].

Reference [4] points out that the integrated LC structure determines the main performance of the Planar Integrated EMI Filter. In the production process, if the integrated LC structure parameters are identified accurately, the integrated LC structure can be improved according to the target performance, then the development cycle can be shortened and the development cost can be reduced.

The parameter identification of the integrated LC structure is a typical multi-peak problem [3], and the identification result is easy to fall into the local optimal solution, so it is difficult to obtain real parameter results. Many modern intelligent optimization algorithms try to solve the multi-peak problem [7-9], the most successful of which is the Immune Algorithm evolved from the Genetic Algorithm [10,11]. However, when using these algorithms, the calculation method of the fitness function has not changed, so it cannot completely solve the problem of falling into the local optimal solution.

This paper proposes an improved Immune Algorithm based on the Feature Selective Validation (FSV) method, which can make the fitness function change continuously during the iteration process, in order to completely solve the problem of falling into the local optimal solution.

The paper is organized as follows: Section II introduces the problem of LC structural parameter identification of the planar integrated EMI filter briefly. Parameter identification based on common Immune Algorithm is presented in Section III. Section IV proposes parameter identification based on improved Immune Algorithm, and its verification is shown in Section V. The conclusions are given in Section VI.

II. PARAMETER IDENTIFICATION PROBLEM OF INTEGRATED LC STRUCTURE

The planar integrated EMI filter is composed of the EI type magnetic core, the integrated Differential Mode (DM) capacitor, the integrated LC module and the

Submitted On: July 27, 2020
Accepted On: November 30, 2020
https://doi.org/10.47037/2020.ACES.J.360103

leakage layer, as shown in Fig. 1. It is the integrated LC structure that plays a decisive role in its performance, as shown in Fig. 2. The integrated LC structure uses printed circuit board manufacturing technology to form winding conductors on both sides of the substrate with a higher dielectric constant, and distributed capacitance will be generated between the upper and lower conductors. At the same time, the magnetic core with higher magnetic permeability will cause inductance in the winding conductor. The dielectric constant of the dielectric layer and the geometric properties of the wire will affect the integrated capacitance parameter, and the magnetic core permeability and the number of coil turns will affect the integrated inductance parameter.

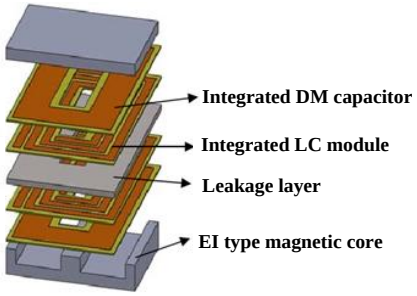

Fig. 1. Composition of the planar EMI filter.

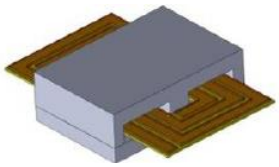

Fig. 2. Integrated LC module with magnetic core.

The lumped parameter model shown in Fig. 3 is used to describe the electrical properties of the integrated LC structure, and then the analysis of high-frequency filtering characteristics can be realized [4]. R represents the loss resistance of the connecting wire, and L is the inductance of the connecting wire. M represents the coupling inductance between the upper and lower conductors, C is the concentrated capacitance to approximate the distributed capacitance between the equivalent layers, and C_p is the parasitic capacitance between turns.

In order to identify the parameter values in the model, four impedance characteristic test experiments are designed under four working conditions. The schematic diagram is shown in Fig. 4.

Case 1: Between terminals B and C is in an open circuit, measure the impedance between terminals A and D:

$$Z_{AD} = \frac{1}{2}\left[R + \frac{(L+M)/C_p}{j\omega(L+M)+2/j\omega C_p} + \frac{2}{j\omega C} \right]. \quad (1)$$

Case 2: Between terminals C and D is in an open circuit, measure the impedance between terminals A and B:

$$Z_{AB} = \frac{2Z_2 / j\omega C}{Z_2 + 2/j\omega C}, \quad (2)$$

$$Z_2 = 2\left[R + \frac{(L-M)/C_p}{j\omega(L-M)+1/j\omega C_p} + \frac{2}{j\omega C} \right]. \quad (3)$$

Case 3: Terminals C and D are short-circuited together, and the impedance between terminals A and B is measured:

$$Z_{AB} = \frac{2Z_3 / j\omega C}{Z_3 + 2/j\omega C}, \quad (4)$$

$$Z_3 = 2\left[R + \frac{(L-M)/C_p}{j\omega(L-M)+1/j\omega C_p} \right]. \quad (5)$$

Case 4: Terminals B and C are short-circuited together, and the impedance between terminals A and D is measured:

$$Z_{AD} = \frac{4Z_4 / j\omega C}{Z_4 + 2/j\omega C}, \quad (6)$$

$$Z_4 = 2\left[R + \frac{(L+M)/C_p}{j\omega(L+M)+1/j\omega C_p} \right]. \quad (7)$$

Using the impedance characteristic curve to determine the equivalent lumped parameter model is a parameter identification problem, and the parameters to be identified are the electrical parameters in the model in Fig. 3. Intelligent optimization algorithms can solve this problem. Taking genetic algorithm as an example, the chromosome is the parameters to be identified. The value range of the parameters can be estimated by the length of the PCB board wire, the distance between the boards and the dielectric constant of the medium. The fitness function is the difference between the model calculated impedance curve and the actual measured impedance curve.

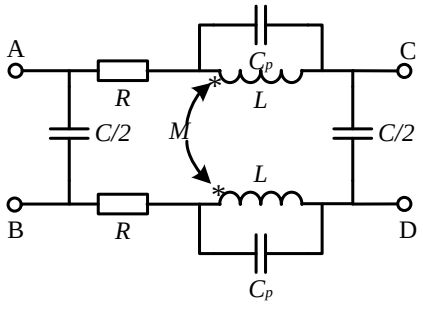

Fig. 3. Lumped parameter model of the integrated LC module [4].

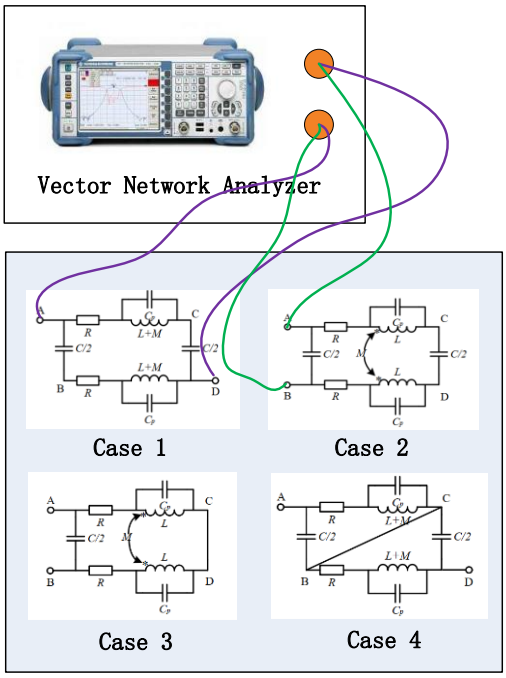

Fig. 4. Schematic diagram of impedance characteristic test experiment.

It is worth noting that different combinations of inductance and capacitance can resonate at the same frequency, so it is easy to fall into a local optimal solution. In other words, parameter identification of integrated LC structure is a multi-peak problem.

III. PARAMETER IDENTIFICATION BASED ON IMMUNE ALGORITHM

In the iterative process of traditional intelligent optimization algorithms, random and unguided searches are performed in the solution space. Although it provides opportunities for evolution, there is inevitably the possibility of degradation. The essential reason for the degradation is that the calculation rule of the fitness function does not change, which will seriously affect the diversity of the solution results. As a result, the identification result converges to the local optimal solution and cannot reach the true global optimal solution.

In the Immune Algorithm, the antibody concentration evaluation operator is introduced according to the concepts of antibodies and antigens in biology. This will avoid the rapid reduction of the diversity of solutions, so as to reduce the possibility of the algorithm falling into the local optimum [11]. The calculation formula of the antibody concentration evaluation operator is arranged as:

$$den(\mathrm{A}_i)=\frac{1}{N}\sum_{j=1}^{N}S(\mathrm{A}_i,\mathrm{A}_j), \tag{8}$$

where A_i represents an antibody consisting of a vector of parameters to be identified, $den(\mathrm{A}_i)$ is the antibody concentration evaluation operator of the antibody A_i. N is the total number of antibodies, and function $S(\mathrm{A}_i,\mathrm{A}_j)$ is represented as:

$$S(\mathrm{A}_i,\mathrm{A}_j)=\begin{cases}1, res(\mathrm{A}_i,\mathrm{A}_j)<\delta\\ 0, res(\mathrm{A}_i,\mathrm{A}_j)\geq\delta\end{cases}. \tag{9}$$

$res(\mathrm{A}_i,\mathrm{A}_j)$ indicates the similarity between two antibodies, usually described by Euclidean distance. δ is the similarity threshold.

Combining the original fitness function value (referred to as the antibody affinity operator in the Immune Algorithm), the incentive calculation operator is obtained according to the following formulas as the final fitness evaluation result of the antibody:

$$sim(\mathrm{A}_i)=a\times aff(\mathrm{A}_i)-b\times den(\mathrm{A}_i), \tag{10}$$

or

$$sim(\mathrm{A}_i)=aff(\mathrm{A}_i)\mathrm{e}^{-a\times den(\mathrm{A}_i)}. \tag{11}$$

Where $aff(\mathrm{A}_i)$ is the antibody affinity operator, a and b are constants determined based on actual calculation.

In this paper, the antibody affinity operator $aff(\mathrm{A}_i)$ is given by FSV method [12,13]. The FSV method is an automated validation method recommended by IEEE Standard 1597.1/2, in order to quantitatively evaluate the difference between Computational Electromagnetics (CEM) simulation results and the reference data. The reference data are the actual measurement results provided according to the Fig. 4.

The main idea of the FSV is shown in Fig. 5. Fourier transform decomposes simulation results and the reference data into three kinds of data with different frequency components. The Amplitude Difference Measure (ADM) is reconstructed from the difference of low frequency data, and the Feature Difference Measure (FDM) is reconstructed from the difference of high frequency data. The Global Difference Measure (GDM) is the final quantitative evaluation value, which combines the results of the ADM and the FDM. The smaller the difference, the smaller the value of GDM, which indicates that the CEM simulation results are better. In this case, the $aff(\mathrm{A}_i)$ is provided as:

$$aff(\mathrm{A}_i)=\sum_{k=1}^{3}FSV_{GDM}\left[Test_{Z_k},Cal_{Z_k}(\mathrm{A}_i)\right], \tag{12}$$

where $Cal_{Z_k}(\mathrm{A}_i)$ means the impedance calculation of the antibody A_i according to the equations from (1) to (5). $Test_{Z_k}$ is the measured result provided by the Impedance Analyzer, and FSV_{GDM} means the GDM value given by the FSV method.

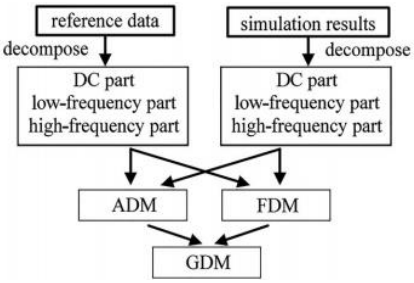

Fig. 5. Main idea of the FSV method [12].

There are four working conditions in Fig. 4. In this paper, the first three working conditions are used to perform the parameter identification as the training set. Then the Case 4 will be treated as the testing set in order to verify the accuracy of the identification results. Thus, the $aff(\mathrm{A}_i)$ result in equation (12) is the sum of the three GDM values.

Noteworthy, only the amplitude results of impedance are applied for the parameter identification in the equation (12), and the phase results are not used.

In the Immune Algorithm, the antibody concentration evaluation operator increases the possibility of antibody mutation, and improves the probability of the algorithm jumping out of the local optimal solution. However, the calculation rule of the antibody affinity operator has not changed, so it has not completely solved the problem of falling into the local optimal solution.

IV. PARAMETER IDENTIFICATION BASED ON IMPROVED IMMUNE ALGORITHM

This section proposes an improved Immune Algorithm, which makes the value of the antibody affinity operator continuously change with the increase of genetic algebra, in order to completely solve the problem of falling into a local optimal solution.

In the FSV method, the GDM is calculated by the ADM and the FDM. The formula is presented as:

$$GDM = \sqrt{\left(k_{ADM} \cdot ADM\right)^2 + \left(k_{FDM} \cdot FDM\right)^2}, \quad (13)$$

where k_{ADM} and k_{FDM} are the weights of ADM and FDM respectively, they are between 0 and 1. Reference [12] gives the weight assignment rules in the standard FSV method.

According to the above properties, the values of k_{ADM} and k_{FDM} can be changed in the iterative process, so that the calculation result of the antibody affinity operator $aff(\mathrm{A}_i)$ is constantly changing during the algorithm implementation process. In this paper, the following weight assignment rule is proposed as:

$$k_{ADM} = 0.2 + 0.8 \times (1 - \frac{gen}{M_{gen}}), \quad (14)$$

and

$$k_{FDM} = 0.2 + 0.8 \times \frac{gen}{M_{gen}}. \quad (15)$$

Where *gen* represents the ongoing genetic algebra, and M_{gen} is total genetic algebra.

Noteworthy, according to the principle of immune algorithm, the larger the gap between parameter 0.2 and 1, the more drastic the fitness function changes, and the easier it is to jump out of the local optimal solution. After testing, the minimum gap required to identify the problem in this article is 0.6, in other words, the parameters can be 0.4 and 1.0. Meanwhile, the algorithm needs to ensure a certain stability in the later stage of the iteration, so the weight parameters are set to 0.2 and 1.0.

In the early stage of the algorithm for parameter identification, ADM plays a decisive role in calculating the result of the antibody affinity operator, while FDM plays a major role in the later stage. This means that the difference in amplitude can be continuously adjusted in the early stage of identification, and the difference in details can be continuously adjusted in the later stage, which fully meets the expectations of evolutionary algorithms.

Most importantly, this method keeps the calculation rule of the antibody affinity operator changing during the iteration. In this way, the diversity of antibodies in the Immune Algorithm can be maintained to the greatest extent, and it is easier to jump out of the local optimal solution to achieve the global optimal solution.

V. ALGORITHM VALIDITY VERIFICATION

In order to verify the accuracy of the proposed method, the real object is produced for providing the standard data, shown as Fig. 6.

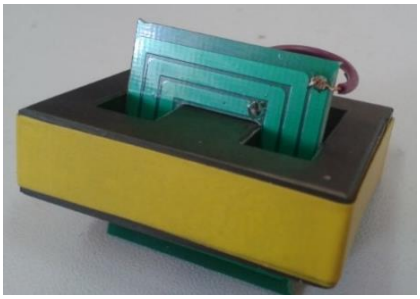

Fig. 6. Physical image of integrated LC module.

The shape of the magnetic core is EE type. The material of the dielectric layer is FR-4, and its thickness is 0.8mm. For the wire related parameters, the number of turns is 3 with the width 2mm. The spacing between the wires is 0.5mm, and the thickness of the wires is $35\mu m$.

A. Parameter identification results based on the experimental data of Case 1, Case 2 and Case 3

As shown in the lumped parameter model in Fig. 3, there are five parameters to be identified, namely C, C_p, L, M and R. Therefore, the dimension of the antibody in the Immune Algorithm is 5. The total number of antibodies is 200, and the maximum immune generation is 150.

The search range of some parameters to be evaluated can be estimated based on the actual LC structure, such as C is from 1×10^{-11}F to 10×10^{-11}F, C_p is from 1×10^{-13}F to 10×10^{-13}F, and L is from 1×10^{-8}H to 10×10^{-8}H. Other parameters can only be estimated based on engineering experience, such as M is from 0H to 10×10^{-9}H, and R is from 0Ω to 10×10^{-3}Ω.

The incentive calculation operator is finally selected as formula (10), in which both a and b are assigned 1. According to the first three working conditions, the parameter identification based on the improved Immune Algorithm is completed, in which the impedance characteristic frequency range is from 10MHz to 1GHz. The antibody affinity operator is the sum of three GDM values from the comparison of the difference between model calculation results and actual measurement results. In the improved Immune Algorithm, it is worth noting that the GDM values are calculated by formula (13) and formula (14).

The identification results of the improved Immune Algorithm are C=4.4×10^{-11}F, C_p=5.8×10^{-13}F, L=6.6×10^{-8}H, M=1.4×10^{-10}H and R=8.7×10^{-6}Ω. For comparison, the identification results of the common Immune Algorithm are C=4.0×10^{-11}F, C_p=5.2×10^{-13}F, L=7.2×10^{-8}H, M=5.3×10^{-10}H and R=3.2×10^{-6}Ω.

The comparison of the results under the three working conditions is given in Fig. 7, Fig. 8 and Fig. 9. The red line represents the actual impedance characteristic curve from the measurement, the black line represents the impedance characteristic curve formed by the Immune Algorithm identification results, and the blue line represents the impedance characteristic curve formed by the identification results of the improved Immune Algorithm.

Using the FSV method, the accuracy of the identification results of the Immune Algorithm and the improved Immune Algorithm can be compared, as shown in Table 1. It shows that the improved Immune Algorithm is more accurate. It also means that the identification result of Immune Algorithm is the local optimal solution, while the improved Immune Algorithm is the global optimal solution. Meanwhile, Table 2 shows the comparison of average relative errors, and it can also give the same conclusion obviously.

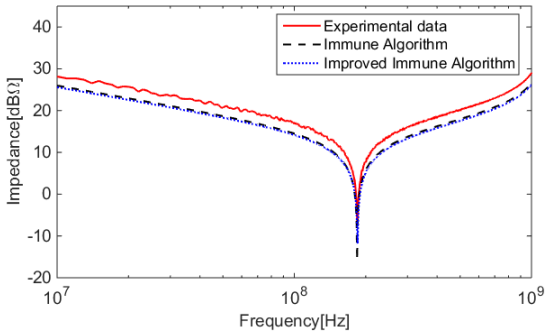

Fig. 7. Comparison of impedance simulation results in Case 1.

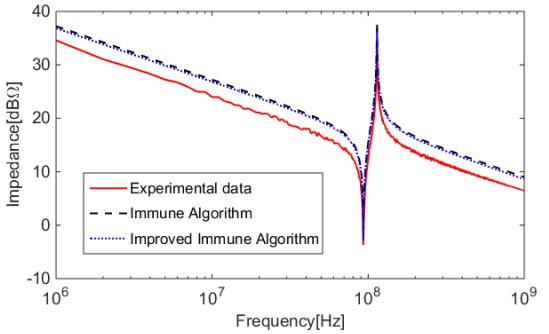

Fig. 8. Comparison of impedance simulation results in Case 2.

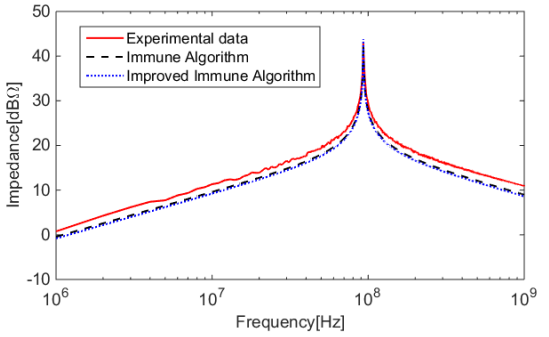

Fig. 9. Comparison of impedance simulation results in Case 3.

Table 1: FSV values for verifying algorithm accuracy

	Immune Algorithm	**Improved Immune Algorithm**
Case 1	0.24	0.23
Case 2	0.20	0.19
Case 3	0.22	0.22
Total	0.66	0.64

Table 2: The comparison of average relative errors

	Immune Algorithm	Improved Immune Algorithm
Case 1	12.27%	12.98%
Case 2	22.83%	19.94%
Case 3	13.36%	15.02%
Mean	16.15%	15.98%

Figure 10 shows the change of the fitness function of the improved Immune Algorithm in the iterative process. This property determines that the proposed method is easier to jump out of the local optimal solution than the common Immune Algorithm. Furthermore, the red line shows that the common Immune Algorithm has converged around the 90th generation, indicating that the selection of the number of chromosomes and genetic algebra is appropriate.

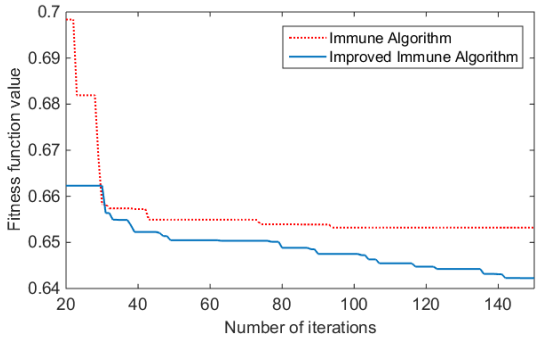

Fig. 10. Change of fitness function in iterative process.

B. Algorithm validity verification according to the experimental data of Case 4

The comparison of the results under the fourth working condition is given in Fig. 11. Meanwhile, Fig. 12 provides the local zoom results of Fig. 11. It is shown that the improved Immune Algorithm is more accurate than the Immune Algorithm.

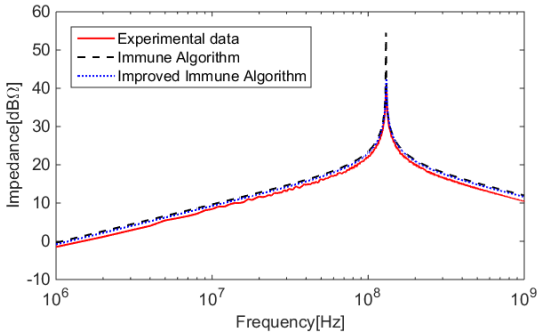

Fig. 11. Comparison of impedance simulation results in Case 4.

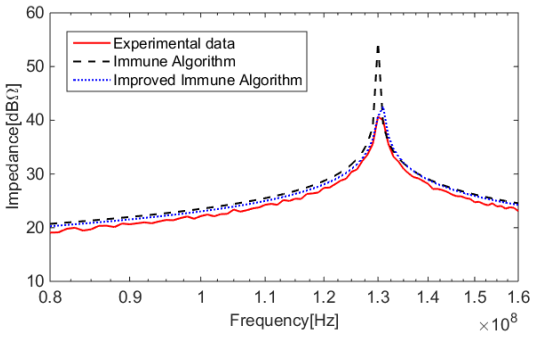

Fig. 12. Local zoom results of Fig. 11.

Using the FSV method, the GDM of the common Immune Algorithm is 0.22, and that of the improved Immune Algorithm is 0.18. Meanwhile, the average relative error of the common Immune Algorithm is 10.43%, and that of the improved Immune Algorithm is 7.06%. It means that the identification results provided by the improved Immune Algorithm are more accurate.

VI. CONCLUSION

Base on the FSV method, this paper proposes an improved Immune Algorithm, in order to solve multi-peak parameter identification problem. Take the parameter identification problem of the integrated LC structure in the Planar Integrated EMI Filter as an example, it is proved that the proposed method is more accurate, because it is easier to jump out of the local optimal solution than the common Immune Algorithm. This achievement not only helps to improve the high-frequency characteristics of the Planar Integrated EMI Filter, but also reduces its manufacturing cost.

ACKNOWLEDGMENT

This work was supported by the Fundamental Research Funds for the Central Universities under Grant 3132020105.

REFERENCES

[1] R. Chen R, J. D. Van Wyk, S. Wang, and W. G. Odendaal, “Planar electromagnetic integration technologies for integrated EMI filters,” *Industry Applications Conference*, pp. 1582-1588, 2003.

[2] R. Chen, J. D. Van Wyk, S. Wang, and W. G. Odendaal, “Improving the characteristics of integrated EMI filters by embedded conductive layers,” *IEEE Transactions on Power Electronics*, vol. 20, no. 3, pp. 611-619, 2005.

[3] H. Huang, L. Deng, B. Hu, and G. Wei, “Techniques for improving the high-frequency performance of the planar CM EMI filter,” *IEEE Transactions on Electromagnetic Compatibility*,

vol. 55, no. 5, pp. 901-908, 2013.

[4] S. Wang and C. Xu, "Extraction of magnetic parameters for elements of a planar EMI filter," *IEEE Transactions on Electromagnetic Compatibility*, vol. 56, no. 2, pp. 360-366, 2014.

[5] J. S. N. T. Magambo, R. Bakri, X. Margueron, P. L. Moigne, A. Mahe, S. Guguen, and T. Bensalah, "Planar magnetic components in more electric aircraft: Review of technology and key parameters for DC–DC power electronic converter," *IEEE Transactions on Transportation Electrification*, vol. 3, no. 4, pp. 831-842, 2017.

[6] J. L. Kotny, T. Duquesne, and N. Idir, "Modeling and design of the EMI filter for DC-DC SiC-converter," *2014 International Symposium on Power Electronics, Electrical Drives, Automation and Motion*, Ischia, pp. 1195-1200, 2014.

[7] S. Wang, M. Roger, J. Sarrazin, and C. Lelandais-Perrault, "Hyperparameter optimization of two-hidden-layer neural networks for power amplifiers behavioral modeling using genetic algorithms," *IEEE Microwave and Wireless Components Letters*, vol. 29, no. 12, pp. 802-805, 2019.

[8] M. Sato, Y. Fukuyama, T. Iizaka, and T. Matsui, "Total optimization of energy networks in a smart city by multi-swarm differential evolutionary particle swarm optimization," *IEEE Transactions on Sustainable Energy*, vol. 10, no. 4, pp. 2186-2200, 2019.

[9] D. Zhang, X. You, S. Liu, and K. Yang, "Multi-colony ant colony optimization based on generalized Jaccard similarity recommendation strategy," *IEEE Access*, vol. 7, pp. 157303-157317, 2019.

[10] Y. Wang, X. Geng, F. Zhang, and J. Ruan, "An immune genetic algorithm for multi-echelon inventory cost control of IOT based supply chains," *IEEE Access*, vol. 6, pp. 8547-8555, 2018.

[11] B. Mohammadi-Ivatloo, A. Rabiee, and A. Soroudi, "Nonconvex dynamic economic power dispatch problems solution using hybrid immune-genetic algorithm," *IEEE Systems Journal*, vol. 7, no. 4, pp. 777-785, 2013.

[12] A. P. Duffy, A. Orlandi, and G. Zhang, "Notice of retraction: Review of the feature selective validation method (FSV). Part I—Theory," *IEEE Transactions on Electromagnetic Compatibility*, vol. 60, no. 4, pp. 814-821, 2018.

[13] A. Orlandi, A. P. Duffy, and G. Zhang, "Notice of retraction: Review of the feature selective validation method (FSV). Part II - Performance analysis and research fronts," *IEEE Transactions on Electromagnetic Compatibility*, vol. 60, no. 4, pp. 1029-1035, 2018.